**Supporting Information**

# Multi-compartment supracapsules made from nano-containers towards programmable release

*Minghan Hu,*[1] Nico Reichholf,[1] Yanming Xia,[2,3] Laura Alvarez,[1] Xiaobao Cao,[2] Shenglin Ma,[3] Andrew J. deMello,[2] Lucio Isa*[1]*

[1] Laboratory for Soft Materials and Interfaces, Department of Materials, ETH Zürich, Vladimir-Prelog-Weg 5, 8093 Zürich, Switzerland

[2] Institute for Chemical and Bioengineering, Department of Chemistry and Applied Biosciences, ETH Zürich, Vladimir-Prelog-Weg 1, 8093 Zürich, Switzerland

[3] Department of Mechanical & Electrical Engineering, Xiamen University, Xiamen, Fujian, China

The supporting information includes: (1) experimental section, (2) additional results, and (3) Videos captions.

## 1. Experimental Section

*Materials*

All chemicals were used as received without further purification: dextran from Leuconostoc spp. ($M_r$ ≈ 6000 Da, Sigma-Aldrich), toluene 2,4-diisocyanate (TDI, Sigma-Aldrich, ≥98.0%) phosphate-buffered saline solution (PBS, pH 7.4, Gibco, Life Technologies Europe, UK), polyglycerol polyricinoleate (PGPR, Danisco, DuPont), cyclohexane (VWR Chemicals BDH, ≥99.9%), sulfo-cyanine-5 carboxylic acid (Cy5, Lumiprobe, $M_w$ = 519 Da), Cy5 conjugated with polyethylene glycol (Cy5-PEG, Biochempeg, $M_w$ ≈ 5000 Da), fluorescein isothiocyanate conjugated with polyethylene glycol (FITC-PEG, Biochempeg, $M_w$ ≈ 5000 Da), and superparamagnetic $Fe_3O_4$ nanoparticles (d = 10 nm, EMG 705, Ferrotec).

*Synthesis of dextran-based nanocapsules*

Nanocapsules were prepared by a polyaddition reaction in an inverse miniemulsion.[1, 2] In a typical experiment, 100 mg dextran and encapsulated cargoes were dissolved in 1 mL of phosphate-

buffered saline solution (pH = 7.4) as the aqueous phase. Depending on the experiment, the encapsulated cargoes were of Cy5, Cy5-PEG, FITC-PEG, or superparamagnetic $Fe_3O_4$ nanoparticles. The concentration of dye and nanoparticles was 1 mg/mL and 5 mg/mL, respectively. The oil phase contained 0.1 g of PGPR as the surfactant in 10 ml of cyclohexane. The water phase and oil phase were mixed and vortexed for 2 minutes to form a pre-emulsion. Subsequently, the pre-emulsified mixture underwent an ultrasonication process to form the final miniemulsion. Typically, ultrasonication was applied for 5 minutes at 40% amplitude with a 20 second pulse and 10 second pause cycle (500 W with 6.24 mm tip probe diameter, Q500, Fisher Scientific, USA) within an ice-bath.

The prepared water-in-oil miniemulsion was stirred at 500 rpm. The crosslinker solution containing 82 µL of TDI and 918 µL of cyclohexane was added dropwise into this stirred miniemulsion over 2 minutes. Afterwards, the polyaddition reaction was carried out at room temperature over 20 hours (**Figure S1**). Synthesized nanocapsule suspensions were centrifuged (500 RCF for 15 minutes) and cyclohexane was replaced three times to remove excess TDI and PGPR. Transfer of the nanocapsules from cyclohexane into water suspension was performed using the following procedure: 1 mL of the nanocapsule dispersion in cyclohexane was mixed with 4 mL of SDS solution (0.2 wt. %) under mechanical stirring (1400 rpm) for at least 4 hours in a fume hood to evaporate cyclohexane. The morphology of nanocapsules was characterized using scanning and the cryo-transmission electron microscopy (SEM and cryo-TEM, Hitachi SU8000 and JEOL JEM1400 respectively).

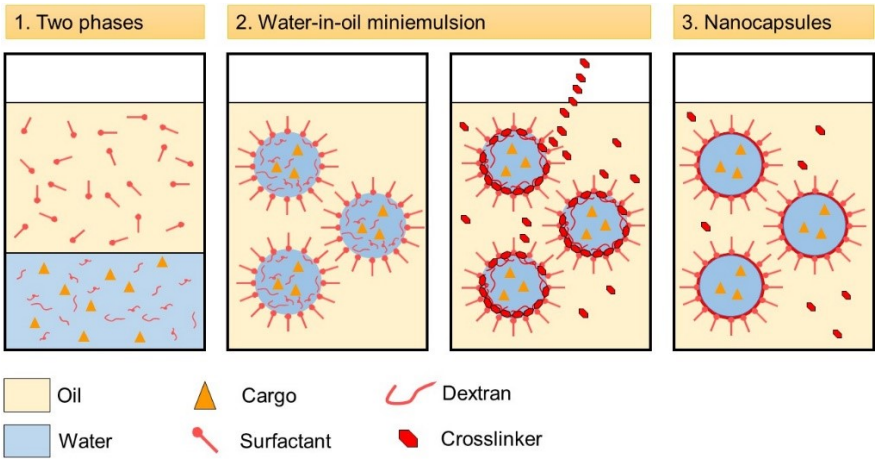


**Figure S1**. Scheme of the synthesis of dextran-based nanocapsules by a polyaddition reaction at the interface of water droplets in a water-in-oil miniemulsion.

*Fabrication of microfluidic devices*

To fabricate droplets of monodisperse size, microfluidics devices containing a cross-junction were designed and fabricated (**Figure S2a**). Briefly, a 2 μm thick photoresist layer (AZ5214, Microchem, USA) was spin-coated onto a 4-inch silicon (Si) wafer at 2000 rpm and then baked for 90 seconds at 95 ℃ on a hotplate. Next, Si wafer with photoresist layer was exposed in a mask aligner (MA6, SUSS, Germany) with 50 $mW/cm^2$. After developing the photoresist in a developer solution (AZ326MIF, Microchem, USA) for 50 seconds and hard-baking for 180 seconds at 110 ℃ on a hotplate, the patterned photoresist was used as a soft mask for the dry etching of silicon. The silicon wafer was vertically etched by deep reactive-ion etching (DRIE) in an ICP etching machine (ICP-Plasma Etcher SI500, Sentech, Germany) to a depth of 11 μm. Microfluidic channels in silicon were obtained after removal of the photoresist by acetone (**Figure S2b**). The remaining organic residues on Si wafer were removed by immersion of Si wafer in a mixture of $H_2SO_4$ and $H_2O_2$ (1:3 v/v) for 15 minutes on a hotplate at 250 ℃. The etched Si wafer was put into a diffusion furnace (5000 Series, Thermco, UK) to deposit a uniform 100 nm thick $SiO_2$ film on the bottom and sidewalls of the microfluidic channels via thermal oxidation (**Figure S2c**). Next, a 3 μm thick photoresist (AZ4620, Microchem, USA) layer was spray-coated on all surfaces of the microfluidic channels using a spray-coating machine (UAM4000L, Cheersonic, China), with a view to preventing the corrosion of the $SiO_2$ film by the $SiO_2$ polishing liquid (**Figure S2d**). The top surface of the silicon wafer with 4 μm thick was removed and polished (including 3 μm spray-coated photoresist and 1 μm silicon layer) using a chemical-mechanical polishing machine (FD-610LP, Fangda Grinder, China) to expose the Si surface (**Figure S2e**). Inlet and outlet holes were machined by laser-drilling on a 4-inch Borofloat 33 glass wafer. Subsequently, the drilled glass was immersed into an HF solution for 30 seconds to remove the processing burrs from laser-drilling (**Figure S2f**). After immersion in the mixture of $H_2SO_4$ and $H_2O_2$ (1:3 v/v) for 15 minutes on a hotplate at 250 ℃, the silicon and glass wafers were aligned and anodically bonded using a wafer-level bonding machine (SB6, SUSS, Germany) (**Figure S2g**). Finally, the bonded glass-silicon devices were diced into small (26 × 15 mm) chips using a wafer dicing saw (DAD321, DISCO, Japan).

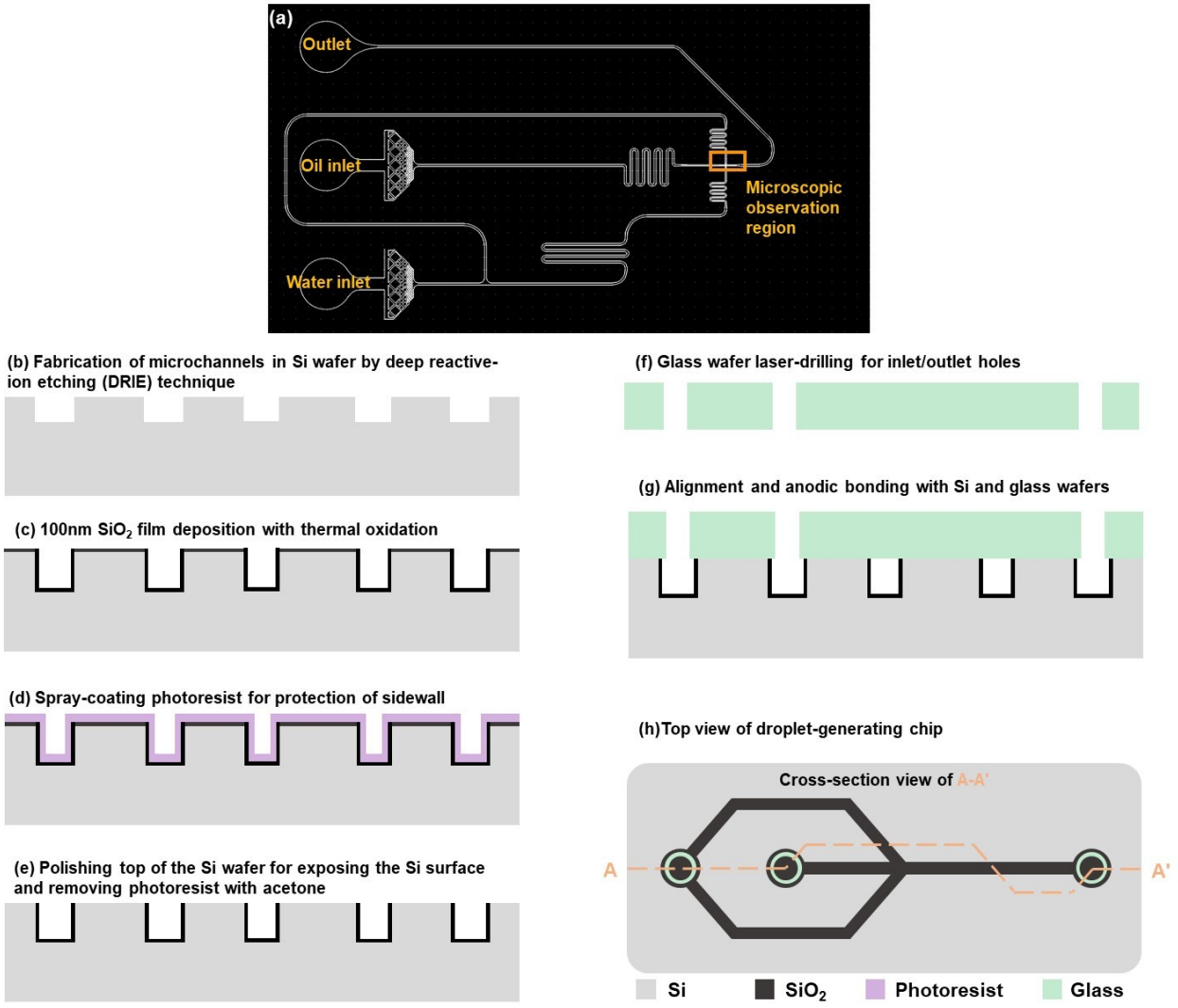


**Figure S2**. Design of the microfluidic chip (a) and the scheme of fabrication process (b - h).

*Cryogenic scanning electron microscope (cryo-SEM)*

5 µl of supracapsules were first vortexed for 30 seconds and then filled into a 6 mm aluminium-planchette, with another aluminium-planchette being used as a lid. The planchette sandwiches were frozen in a high-pressure freezer (HPM 100, Bal-Tec/Leica, Austria) and stored in liquid nitrogen. Vitrified specimens were then transferred and mounted under liquid nitrogen on a cryo-holder and finally transferred under liquid nitrogen into a precooled (-130°C) freeze-fracturing system (BAF 060, Bal-Tec/Leica, Austria) at $1.10^{-6}$ mbar. Coating was performed with 3 nm tungsten at an elevation angle of 45° followed by 3 nm at 90°. Transfer to the precooled cryo-SEM was done under high vacuum ($< 5 \times 10^{-6}$ mbar) with an air-lock shuttle. Cryo-SEM was performed

in a field emission SEM (Leo Gemini 1530, Carl Zeiss, Germany) equipped with a cold stage to maintain the specimen temperature at -120 °C (VCT Cryostage, Bal-Tec/Leica, Austria).

*Cryogenic transmission electron microscopy (TEM)*

For cryo-TEM analysis, 3.8 µl of a nanocapsule water suspension was deposited on a Lacey carbon-coated 300-mesh copper grid (Quantifoil Micro tools GmbH, Germany), which was previously negatively glow-discharged at 25 mA for 45 seconds. Excess sample was blotted away for 2 seconds and the grid plunge-frozen in a liquid ethane/propane mixture (continuously cooled by liquid nitrogen) using an automated vitrification system (Vitrobot Mark IV, Thermo Fisher Scientific, USA) with the environmental chamber set to 100% humidity and 22°C. Vitrified grids were fixed in Titan cartridges (Thermo Fischer Scientific, USA) and observed under an electron microscope (Titan Krios G, Thermo Fischer Scientific, USA) using a cryo-holder (Gatan 626, Gatan Inc, USA).

*Magnetic properties of nanocapsules and supracapsules*

The mangentic properties of nanocapsules and supracapsules were characterized by a vibrating sample magnetometry (PPMS Model 6000, QuantumDesign, Germany). The nanocapsules and supracapsules were first dried in an oven at 70ºC for overnight to obtain powder. Then the powder sample was weighted and attached on a Kapton tape (DuPont, USA) then finally mounted on a quartz glass sample holder. It was continuously measured at 300 K and 40 Hz while the magnetic field was varied from 0 T – 2 T – -2 T – 2 T – 0 T at 1 mT/s. The diamagnetic response from the sample holder and Kapton tape was subtracted by a reference measurement of the holder and tape without sample.

*Rotation magnetic motion of supracapsules*

5 µl of a supracapsule dispersion made with magnetic nanocapsules (diameter is 7.4 µm, 0.1 wt. %) was dispersed between two transparent thin glass slides (85 – 115 µm thickness, Menzel Glaser, Germany) in a 9 mm-circular reservoir with a 0.12 mm-thick sealing spacer (Grace Bio-Labs SecureSeal, US). We applied a rotating magnetic field in the plane of the sample using a custom-built setup fitted with two pairs of independent Helmholtz coils.[3] The magnetic field was constant within a few percent over a 1 $mm^2$ area in the center of the cell, and the maximum applicable

magnetic field was 65 mT. In experiments, we used a field of 40 mT to actuate particles. The sample was imaged in transmission using a 10× long-working distance objective and snapshots were recorded with a CCD camera at 10 frames per second. The recorded image sequences were then analysed using custom Matlab codes in order to extract the positions of the supraparticles in each frame.

## 2. Additional Results

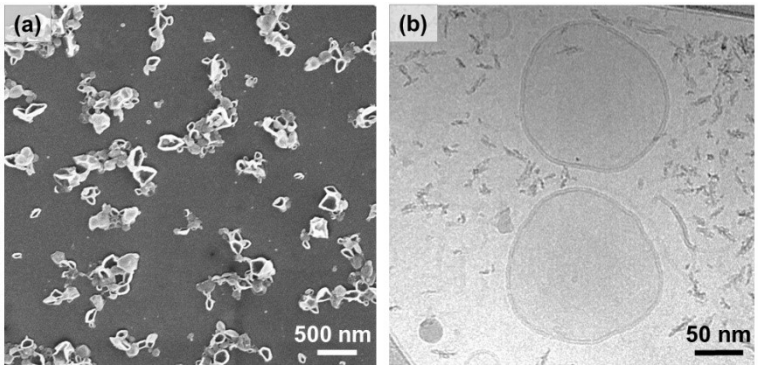


**Figure S3**. SEM (a) and cryo-TEM (b) of synthesized dextran-based nanocapsules

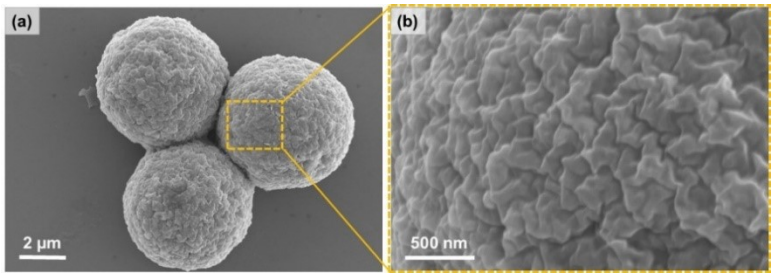


**Figure S4**. SEM images of supracapsules (a) and their zoomed-in surface morphology (b).

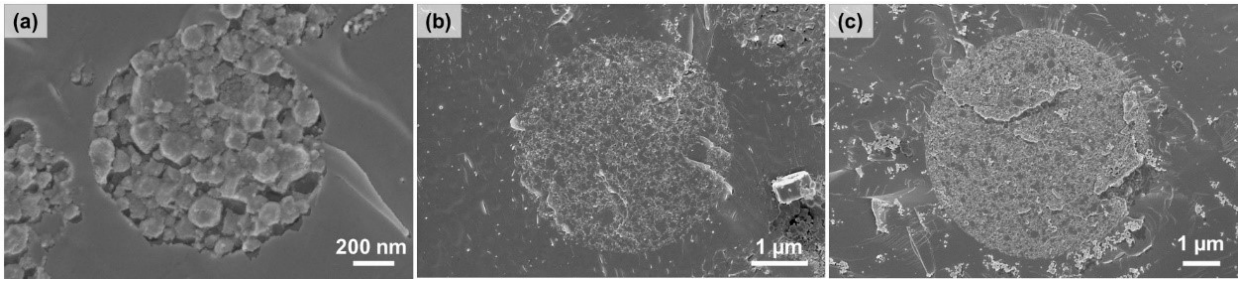


**Figure S5**. Cryo-SEM images of cross-sections of the supracapsules with diameters of 5 µm (a), 12 µm (b), and 16 µm (c).

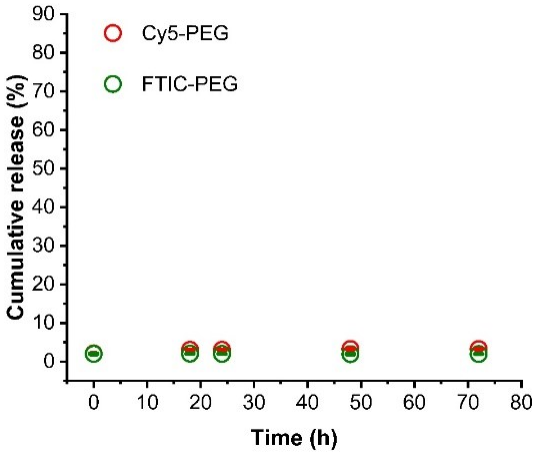


**Figure S6**. Release profiles of fluorescent dyes from supracapsules assembled from three types of nanocapsules containing different cargoes: Cy5-PEG (red), FITC-PEG (green) and water in a 1:1:3 volume ratio.

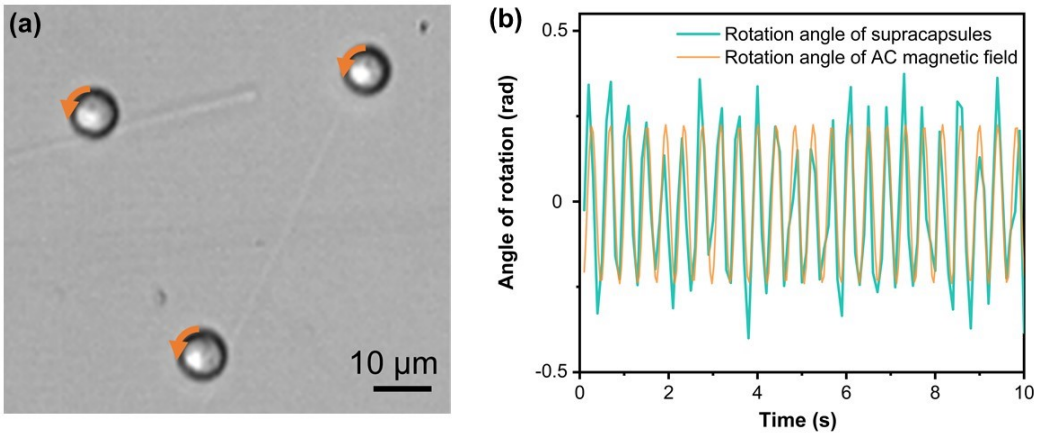


**Figure S7**. Controlled rotation motion of magnetic supracapsules by applying an oscillating magnetic field. (a) Optical microscopy images indicating the rotation angle (30°) of magnetic supracapsules. (b) Rotation angle of magnetic supracapsules under an oscillating magnetic field.

**Table S1**. Droplet size as a function of flow rates in a cross-junction microfluidic device (see Figure S2a)

| Diameter [μm] | Oil inlet [μL/min] | Water inlet [μL/min] | Volume fraction of nanocapsules |
|---|---|---|---|
| 15.4 ± 0.8 | 2.0 | 25.0 | 0.032 |
| 16.6 ± 0.1 | 0.5 | 5.0 | 0.009 |
| 18.8 ± 0.4 | 2.0 | 10.0 | 0.032 |
| 19.2 ± 0.1 | 0.5 | 5.0 | 0.024 |
| 23.5 ± 0.1 | 1.0 | 5.0 | 0.009 |
| 23.9 ± 0.8 | 2.5 | 8.0 | 0.032 |
| 23.9 ± 0.1 | 1.0 | 5.0 | 0.024 |
| 24.7 ± 0.4 | 2.0 | 6.0 | 0.071 |
| 24.8 ± 0.2 | 2.0 | 5.0 | 0.024 |
| 25.9 ± 1.0 | 2.5 | 6.0 | 0.071 |
| 27.6 ± 0.4 | 4.0 | 5.0 | 0.024 |
| 28.0 ± 0.2 | 3.0 | 5.0 | 0.009 |

We note that the droplet size does not only depend on the flow rates in oil and water inlets, but also changes with the volume fraction of nanocapsules within the droplets.

**Table S2**. Effective diffusion coefficient and half-life time of dye release from nanocapsules and supracapsules

| | Diameter [μm] | Diffusion coefficient [$m^2/s$] | Half-life time of dye release [h] |
|---|---|---|---|
| Nanocapsules | 0.2 | $4.85 \times 10^{-22}$ | 0.69 |
| Small supracapsules | 5 | $2.49 \times 10^{-22}$ | 1.14 |
| Medium supracapsules | 12 | $1.63 \times 10^{-22}$ | 1.99 |
| Big supracapsules | 16 | $1.02 \times 10^{-22}$ | 3.41 |

## 3. Supporting Videos

Video S1. Demonstration of the magnetic response of a suspension of superparamagnetic supracapsules.

Video S2. Magnetically controlled motion of a superparamagnetic supracapsule. Scale bar is 50 μm.

## 4. References

1. Alkanawati, M. S.; da Costa Marques, R.; Mailänder, V.; Landfester, K.; Thérien-Aubin, H., Polysaccharide-Based pH-Responsive Nanocapsules Prepared with Bio-Orthogonal Chemistry and Their Use as Responsive Delivery Systems. *Biomacromolecules* **2020,** *21* (7), 2764-2771.
2. Alkanawati, M. S.; Machtakova, M.; Landfester, K.; Thérien-Aubin, H., Bio-Orthogonal Nanogels for Multiresponsive Release. *Biomacromolecules* **2021,** *22* (7), 2976-2984.
3. Buttinoni, I.; Zell, Z. A.; Squires, T. M.; Isa, L., Colloidal binary mixtures at fluid–fluid interfaces under steady shear: structural, dynamical and mechanical response. *Soft Matter* **2015,** *11* (42), 8313-8321.